Numerical validation of a $\kappa-\epsilon-\kappa_\theta-\epsilon_\theta$ heat transfer turbulence model for heavy liquid metals

2015 J. Phys.: Conf. Ser. 655 012046

(http://iopscience.iop.org/1742-6596/655/1/012046)

Numerical validation of a κ-ω-κ_θ-ω_θ heat transfer turbulence model for heavy liquid metals

D Cerroni[1], R Da Vià[1], S Manservisi[1], F Menghini[1], G Pozzetti[2] and R Scardovelli[1]

[1] DIN - Lab. of Montecuccolino, University of Bologna, Via dei Colli 16, 40136 Bologna, Italy
[2] RUES, University of Luxemburg, 6, rue Richard Coudenhove-Kalergi, L-1359 Luxembourg

E-mail: `filippo.menghini3@unibo.it`

Abstract. The correct prediction of heat transfer in turbulent flows is relevant in almost all industrial applications but many of the heat transfer models available in literature are validated only for ordinary fluids with $Pr \simeq 1$. In commercial Computational Fluid Dynamics codes only turbulence models with a constant turbulent Prandtl number of $0.85 - 0.9$ are usually implemented but in heavy liquid metals with low Prandtl numbers it is well known that these models fail to reproduce correlations based on experimental data. In these fluids heat transfer is mainly due to molecular diffusion and the time scales of temperature and velocity fields are rather different, so simple turbulence models based on similarity between temperature and velocity cannot reproduce experimental correlations. In order to reproduce experimental results and Direct Numerical Simulation data obtained for fluids with $Pr \simeq 0.025$ we introduce a κ-ϵ-κ_θ-ϵ_θ turbulence model. This model, however, shows some numerical instabilities mainly due to the strong coupling between κ and ϵ on the walls. In order to fix this problem we reformulate the model into a new four parameter κ-ω-κ_θ-ω_θ where the dissipation rate on the wall is completely independent on the fluctuations. The model improves numerical stability and convergence. Numerical simulations in plane and channel geometries are reported and compared with experimental, Direct Numerical Simulation results and with results obtained with the κ-ϵ formulation, in order to show the model capabilities and validate the improved κ-ω model.

Keywords: Turbulent Heat Transfer, Turbulence Modeling.

1. Introduction

Heavy liquid metals such as mercury, Lead-Bismuth Eutectic (LBE) or sodium-potassium alloys with low Prandtl number are promising coolant fluids for achieving the necessary requirements for the design of fast nuclear reactors. In ordinary fluids such as water or air, similarity between thermal and dynamical fields holds and a Simple Eddy Diffusivity (SED) model coupled with a two-equation turbulence model seems to be sufficient to obtain reliable thermal and dynamical results. On the contrary, in liquid metals with low Prandtl numbers the temperature and velocity time scales are rather different since heat transfer is due to both molecular diffusion and convection. In these fluids the hypothesis of a constant turbulent Prandtl number fails to reproduce experimental correlations [1, 2, 3]. Algebraic expressions for the turbulent Prandtl number depending on turbulent and velocity fields have been recommended by many authors in order to correctly reproduce experimental data with these fluids, but these correlations are geometry dependent and new expressions have to be defined for each studied case [2]. For this reason the SED model and these algebraic expressions should not be used in Computational

Fluid Dynamics (CFD) simulations over new geometrical configurations where no experimental data are available.

In the last several years many turbulence models taking into account thermal turbulence effects have been proposed. These turbulence models have been successfully employed to compute the turbulent heat transfer in ordinary fluids with $Pr \approx 1$ in complicated geometry and detached flows. All of these models use the Algebraic Flux Model (AFM) in implicit or explicit formulation to calculate the turbulent heat flux. In this paper we deal with an explicit formulation of the AFM and compute the turbulent heat flux using a gradient hypothesis with isotropic eddy heat diffusivity α_t. The eddy or turbulent heat diffusivity has to be defined using appropriate time scales for the turbulence modeling. The thermal turbulent time scale is computed by defining the mean square temperature fluctuation κ_θ, its dissipation ϵ_θ and its specific dissipation rate ω_θ which have to be computed using appropriate transport equations. By coupling a low-Reynolds number κ-ϵ system and a κ_θ-ϵ_θ system one can obtain a four parameter turbulence model which solves the averaged Navier-Stokes system and defines the Reynolds stress tensor and the turbulent heat flux [4, 5, 6, 7, 8]. A four parameter turbulence model based on a κ-ϵ formulation has been already proposed by the authors, see [9, 10]. However it was found that this model shows convergence issues mainly due to the coupling of the variables in the boundary conditions. In this paper we propose a new four parameter κ-ω-κ_θ-ω_θ model based on the already tested κ-ϵ-κ_θ-ϵ_θ to overcome these problems. In this model a fixed Dirichlet boundary condition which does not depend on κ can be imposed for ω on the wall. The model is therefore more stable and robust and numerical convergence is faster.

In the next section the two turbulence models are introduced. They consist both of four transport equations, two for the dynamical turbulence modeling and two for the thermal. The derivation of the κ-ω formulation is presented together with a discussion over the new boundary conditions to be set in this model. In the third section the numerical results obtained with the new turbulence model for the simulation of fully developed turbulent flows in plane and cylindrical geometries are reported. These results are compared with the ones obtained with the κ-ϵ model, with Direct Numerical Simulation (DNS), when they are available, and with experimental heat transfer correlations for the evaluation of the Nusselt number Nu as a function of Peclet number Pe. Finally conclusions and remarks are taken over the usefulness of this turbulence model in nuclear engineering applications when heavy liquid metals are employed.

2. Transport equations and turbulence models

Heavy liquid metals can be considered incompressible in nuclear reactor cores, so the Reynolds-averaged incompressible system of Navier-Stokes can be used. It reads

$$\nabla \cdot \mathbf{u} = 0\,, \tag{1}$$

$$\rho \frac{\partial \mathbf{u}}{\partial t} + \rho(\mathbf{u} \cdot \nabla)\mathbf{u} = \nabla \cdot \sigma - \nabla \cdot \tau + \rho \mathbf{g}\,, \tag{2}$$

$$\rho C_p \left(\frac{\partial T}{\partial t} + (\mathbf{u} \cdot \nabla) T \right) = \nabla \cdot \mathbf{q} - \nabla \cdot \mathbf{q}_\theta + Q\,, \tag{3}$$

where $\mathbf{u}$ is the averaged velocity of the fluid and T is the averaged temperature. The tensors σ and $\mathbf{q}$ are the usual viscous stress and heat flux and they are modeled using Navier-Stokes constitutive law for viscous fluids and Fourier law for heat conduction.

$$\sigma := -p\mathbf{I} + \mu \mathbf{D} \quad \text{with} \quad \mathbf{D} := \nabla \mathbf{u} + \nabla \mathbf{u}^T \tag{4}$$

$$\mathbf{q} := -\lambda \nabla T\,. \tag{5}$$

Two new terms appear after the averaging process, namely the Reynolds stress tensor τ and the turbulent heat flux $\mathbf{q}_\theta$, defined as the averaged product of the fluctuating components of velocity with itself and velocity with temperature. These terms are calculated as

$$\tau = \rho\overline{\mathbf{u}'\mathbf{u}'} \quad , \quad \mathbf{q}_\theta = \rho C_p \overline{\mathbf{u}'T'} \,. \tag{6}$$

Instead of solving the transport equations for the Reynolds stress tensor and for the turbulent heat flux we approximate these terms with the eddy diffusivity model as

$$\tau = -\nu_t \left(\nabla\mathbf{u} + \nabla\mathbf{u}^T\right) + \frac{2\kappa}{3}\mathbf{I}\,, \tag{7}$$

$$\mathbf{q}_\theta = -\alpha_t \nabla T\,, \tag{8}$$

where the eddy diffusivity of momentum ν_t and the heat eddy diffusivity α_t must be properly defined in the turbulence model. We assume them as a function of the turbulence kinetic energy κ and two characteristic time scales, namely τ_{lu}, for dynamical turbulence, and $\tau_{l\theta}$, for thermal turbulence. The eddy viscosity and the eddy diffusivity are then defined as

$$\nu_t := C_\mu\, \kappa\tau_{lu}\,, \quad \alpha_t := C_\theta\, \kappa\tau_{l\theta}\,, \tag{9}$$

where $C_\mu = 0.09$ and $C_\theta = 0.1 = C_\mu/0.9$. The ratio between the two eddy diffusivities is defined as the turbulent Prandtl number, which is $Pr_t = \nu_t/\alpha_t$.

2.1. κ-ϵ-κ_θ-ϵ_θ turbulence model

We can define the turbulence kinetic energy κ and its dissipation ϵ as

$$\kappa := \frac{1}{2}\overline{\mathbf{u}'^2} \qquad \epsilon := \nu\overline{\|\nabla\mathbf{u}'\|^2}\,. \tag{10}$$

The equations for κ and for its dissipation ϵ are obtained taking appropriate moments of the Navier-Stokes equations of motion. A modeling of the terms appearing in the equations is needed and the final equation for κ is

$$\frac{\partial\kappa}{\partial t} + (\mathbf{u}\cdot\nabla)\kappa = \nabla\cdot\left[\left(\nu + \frac{\nu_t}{\sigma_\kappa}\right)\nabla\kappa\right] + P_\kappa - \epsilon\,, \tag{11}$$

where

$$P_\kappa := -\overline{u_i'u_j'}\frac{\partial u_i}{\partial x_j} = \frac{\nu_t}{2}\left|\nabla\mathbf{u} + \nabla\mathbf{u}^T\right|^2\,. \tag{12}$$

A similar modeling for ϵ gives the equation [7]

$$\frac{\partial\epsilon}{\partial t} + (\mathbf{u}\cdot\nabla)\epsilon = \nabla\cdot\left[\left(\nu + \frac{\nu_t}{\sigma_\epsilon}\right)\nabla\epsilon\right] + C_{1\epsilon}\frac{\epsilon}{\kappa}P_\kappa - C_{2\epsilon}\frac{\epsilon^2}{\kappa}f_\epsilon\,. \tag{13}$$

with $C_{1\epsilon} = 1.5$, $C_{2\epsilon} = 1.9$, $C_\mu = 0.09$, $\sigma_\kappa = 1.4$, $\sigma_\epsilon = 1.4$, P_κ defined by (12) and f_ϵ

$$f_\epsilon = \left(1 - \exp(-0.3226\,R_\delta)\right)^2\left(1 - 0.3\exp(-0.0237\,R_t^2)\right)\,. \tag{14}$$

By defining the characteristic time $\tau_u = \kappa/\epsilon$ one can model the local dynamical time τ_{lu} in many ways. In this work we use the κ-ϵ model as reported in [9]. This model can reproduce the correct near-wall turbulence behavior, that is $\kappa \propto \delta^2$, $\epsilon \propto \delta^0$ and $\nu_t \propto \delta^3$ for $\delta \to 0$ see [7, 8, 9].

We can define also the mean square temperature fluctuation κ_θ and its dissipation ϵ_θ as

$$\kappa_\theta := \frac{1}{2}\overline{T'^2}\,, \qquad \epsilon_\theta := \frac{\nu}{Pr}\overline{\|\nabla T'\|^2}\,. \tag{15}$$

Two transport equations are needed for these variables and they can be obtained as [11]

$$\frac{\partial \kappa_\theta}{\partial t} + (\mathbf{u}\cdot\nabla)\kappa_\theta = \nabla\cdot\left[(\alpha + \frac{\alpha_t}{\sigma_{\kappa_\theta}})\nabla\kappa_\theta\right] + P_\theta - \epsilon_\theta\,, \tag{16}$$

where

$$P_\theta := -\overline{\mathbf{u}'T'}\cdot\nabla T = \alpha_t\,\|\nabla T\|^2\,. \tag{17}$$

The equation for ϵ_θ can be written as [9, 11]

$$\frac{\partial \epsilon_\theta}{\partial t} + (\mathbf{u}\cdot\nabla)\epsilon_\theta = \nabla\cdot\left[(\alpha + \frac{\alpha_t}{\sigma_{\epsilon_\theta}})\nabla\epsilon_\theta\right] + \frac{\epsilon_\theta}{\kappa_\theta}\Big(C_{p1}\,P_\theta - C_{d1}\,\epsilon_\theta\Big) + \frac{\epsilon_\theta}{\kappa}\Big(C_{p2}\,P_\kappa - C_{d2}\,\epsilon\Big)\,, \tag{18}$$

where P_κ is defined by (12) and P_θ by (17). For heavy liquid metals with $Pr \approx 0.025$ we have used the coefficients defined in [5, 6], namely $C_{d1} = 0.9$, $C_{p2} = 0.9$. The coefficient C_{p1} has been set to 0.925 and

$$C_{d2} = 1.9\,(1 - 0.3\,\exp(-0.0237\,R_t^2))(1 - \exp(-0.0308\,R_\delta))^2\,. \tag{19}$$

For details one can see [4, 11, 12]. As we have done for the dynamical turbulence we can define the thermal time scale as $\tau_\theta = \kappa_\theta/\epsilon_\theta$. The ratio between the turbulent thermal time and the turbulent dynamical time, $R = \tau_\theta/\tau_u$, can be used in order to model the local thermal characteristic time $\tau_{l\theta}$, as reported in [9]. For details one can refer to [4, 7, 8, 11, 13] and references therein.

Having defined the turbulent heat flux and the Reynolds stress tensor the problem is closed and the four parameter system can be solved by assigning appropriate boundary conditions which are discussed in section 2.3.

2.2. κ-ω-κ_θ-ω_θ turbulence model

To obtain a κ-ω formulation of the turbulence model introduced in section 2.1 we define the variables ω and ω_θ, as the specific dissipation rate of κ and κ_θ. These new variables are defined as:

$$\omega = \frac{\epsilon}{C_\mu \kappa}\,, \qquad \omega_\theta = \frac{\epsilon_\theta}{C_\mu \kappa}. \tag{20}$$

By algebraically substituting the definitions (20) in the system of equations (11-13-16-18) we obtain

$$\frac{\partial \kappa}{\partial t} + \mathbf{u}\cdot\nabla\kappa = \nabla\cdot\left[\left(\nu + \frac{\nu_t}{\sigma_k}\right)\nabla\kappa\right] + P_\kappa - C_\mu\,\kappa\,\omega\,, \tag{21}$$

$$\begin{aligned}\frac{\partial \omega}{\partial t} + \mathbf{u}\cdot\nabla\omega = \nabla\cdot\left[\left(\nu + \frac{\nu_t}{\sigma_\epsilon}\right)\nabla\omega\right] + \frac{2}{\kappa}\left(\nu + \frac{\nu_t}{\sigma_\epsilon}\right)\nabla\kappa\cdot\nabla\omega + \\ + (c_{\epsilon 1} - 1)\,\frac{\omega}{\kappa}P_\kappa - C_\mu\,(c_{\epsilon 2} f_\epsilon - 1)\,\omega^2\,,\end{aligned} \tag{22}$$

$$\frac{\partial \kappa_\theta}{\partial t} + \mathbf{u}\cdot\nabla\kappa_\theta = \nabla\cdot\left[\left(\alpha + \frac{\alpha_t}{\sigma_\theta}\right)\nabla\kappa_\theta\right] + P_\theta - C_\mu\,\kappa_\theta\,\omega_\theta\,, \tag{23}$$

$$\begin{aligned}\frac{\partial \omega_\theta}{\partial t} + \mathbf{u}\cdot\nabla\omega_\theta = \nabla\cdot\left[\left(\alpha + \frac{\alpha_t}{\sigma_\theta}\right)\nabla\omega_\theta\right] + \frac{2}{\kappa_\theta}\left(\alpha + \frac{\alpha_t}{\sigma_\theta}\right)\nabla\kappa_\theta\cdot\nabla\omega_\theta + \\ + (c_{p1} - 1)\,\frac{\omega_\theta}{\kappa_\theta}P_\theta + c_{p2}\frac{\omega_\theta}{\kappa}P_\kappa - (c_{d1} - 1)\,C_\mu\omega_\theta^2 - c_{d2}C_\mu\omega\omega_\theta\,.\end{aligned} \tag{24}$$

For the κ-ω turbulence model the coefficients $c_{\epsilon 1}$, $c_{\epsilon 2}$ and the function f_ϵ are the same used in the κ-ϵ model. For the κ_θ-ω_θ thermal turbulence model the coefficient c_{p2} and the function

c_{d2} are the same used in the κ_θ-ϵ_θ model, while c_{p1} and c_{d1} have been set to 1.025 and 1.1. In a κ-ω formulation the time scales of turbulence can be simply computed as $\tau_u = (C_\mu\,\omega)^{-1}$ and $\tau_\theta = (C_\mu\,\omega_\theta)^{-1}$, so the time ratio becomes $R = \omega/\omega_\theta$. Using this model we can avoid the variables coupling in the boundary conditions which occurs in κ-ϵ formulation, as we prove in the following section.

2.3. Boundary conditions for the turbulence models

We can study the near wall behavior of the turbulent variables by using Taylor series expansion near the wall. By applying this expansion to κ, ϵ, κ_θ and ϵ_θ we obtain the following expressions

$$\kappa_w = \frac{1}{2}\,a\,\delta^2, \qquad \epsilon_w = \nu\frac{\kappa_w}{\delta^2}, \qquad \kappa_{\theta w} = \frac{1}{2}\,a_\theta\,\delta^2, \qquad \epsilon_{\theta w} = \alpha\frac{\kappa_{\theta w}}{\delta^2}\,, \tag{25}$$

where δ is the distance from the wall and a and a_θ are constant values that depend on the velocity and temperature fluctuations. In this case we cannot impose exact Dirichlet boundary conditions on ϵ and ϵ_θ because the values κ_w and $\kappa_{\theta w}$ are not known *a priori*. A Neumann boundary condition is imposed for κ and κ_θ while a Dirichlet boundary condition depending on the value of κ and κ_θ as computed in the previous iteration is employed for ϵ and ϵ_θ. This algorithm can lead to convergence issues if oscillations of the solutions on the wall do generate.

The near wall Taylor series expansion of ω and ω_θ is

$$\omega_w = \frac{2\nu}{C_\mu\delta^2}\,, \qquad \omega_{\theta w} = \frac{2\alpha}{C_\mu\delta^2}\,. \tag{26}$$

As can be seen in (26) it is now possible to impose exact Dirichlet boundary conditions for ω and ω_θ near the wall because the terms on the right hand side are known values. In this case we have no coupling between the variables on the wall boundary condition and the solution of this system is more robust and stable. As it can be seen, in both formulations the time scale ratio R on the wall is equal to the molecular Prandtl number of the fluid while the turbulent kinetic energy κ and the mean square temperature fluctuation κ_θ tend to zero on the wall.

3. Numerical results

In the next sections we report the numerical results of fully developed turbulent flow simulations in different geometries. The physical properties of the fluid are reported in Table 1. These properties are representative of Lead-Bismuth-Eutectic and other heavy liquid metal fluids with a molecular Prandtl number of $Pr = 0.025$.

An in-house finite element code is used to solve all the systems of partial differential equations. The code allows to refine the mesh to obtain better resolution using a multigrid solver. We employ Taylor-Hood finite elements for the system of Navier-Stokes in order to satisfy the inf-sup condition and this system is solved with a fully coupled velocity-pressure method. The two systems of turbulence equations are solved with standard quadratic finite elements. All the transport equations are up-winded by a SUPG algorithm to improve the stability of the solution. The solution of the turbulent fields is obtained in two steps: first the dynamical fields are obtained and then the thermal ones are solved.

Physical properties of LBE fluid

Viscosity	μ	0.00184 Pa s
Density	ρ	10340 Kg/m^3
Thermal conductivity	λ	10.72 W/(m K)
Heat specific capacity	C_p	145.75 J/(Kg K)

Table 1. Physical parameters used in the CFD simulations.

Journal of Physics: Conference Series **655** (2015) 012046 doi:10.1088/1742-6596/655/1/012046

3.1. Plane channel

In this section we report numerical results obtained for a fully developed turbulent flows in plane channel geometry. This geometry is chosen because it is very simple and many DNS data are available for this flow. The physical properties of the fluid are reported in Table 1. We

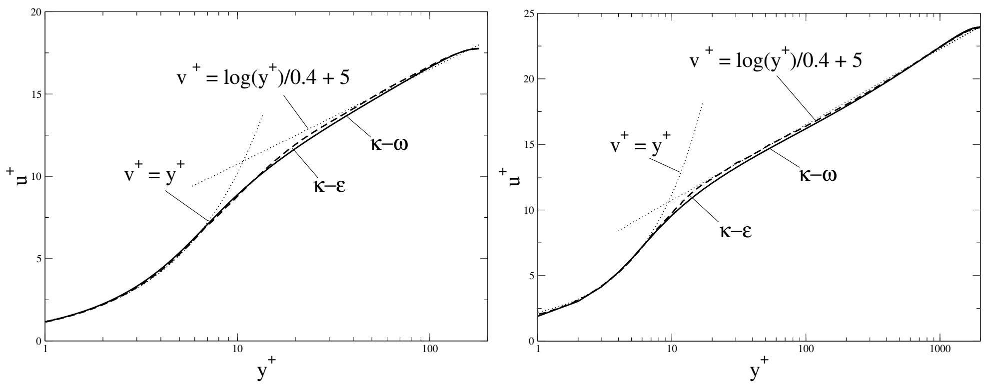

Figure 1. Plane case. Mean velocity distribution for $Re \approx 5500$ (left) and $Re \approx 86200$ (right) as computed with κ-ϵ and κ-ω model.

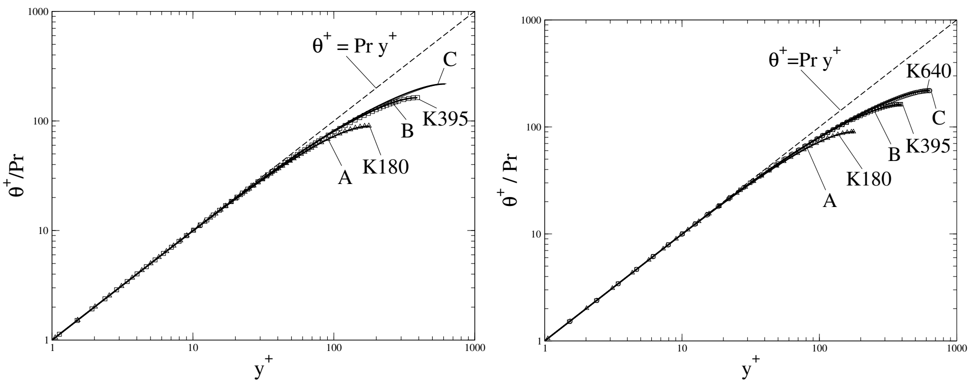

Figure 2. Plane case. Comparison of the temperature distribution θ^+/Pr obtained with κ-ϵ (left) and κ-ω model (right), with DNS data. DNS data are reported for $Re_\tau = 180$ (K180), $Re_\tau = 395$ (K395) and $Re_\tau = 640$ (K640).

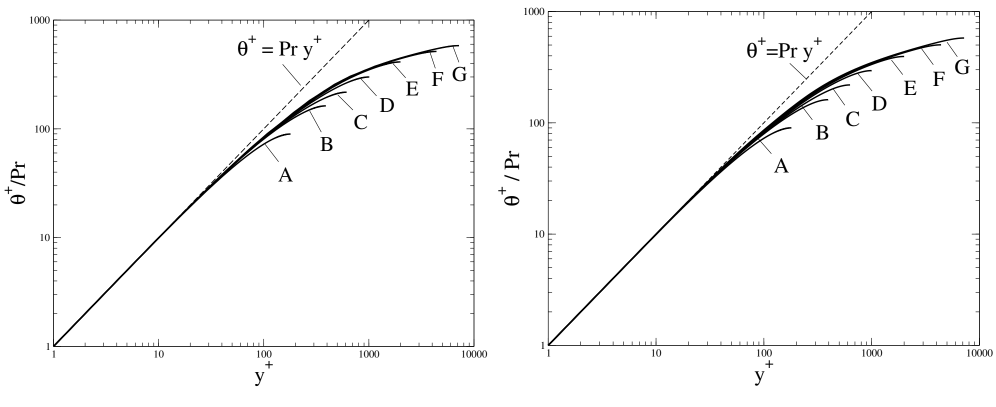

Figure 3. Plane case. Temperature distribution θ^+/Pr for different velocities $Re \approx 5500$ (A), 13500 (B), 23250 (C), 40100 (D), 86200 (E), 203900 (F) and 344800 (G). On the left the results were obtained with the κ-ϵ-κ_θ-ϵ_θ model while on the right the results were obtained with κ-ω-κ_θ-ω_θ model

consider two plates located at a distance $L = 0.0605$ m and with infinite dimensions in the other directions. On the wall a uniform heat flux of 360000 W/m^2 is applied. We can solve this problem in two dimensions with periodic boundary conditions on the inlet and outlet of the channel. The results of the κ-ω-κ_θ-ω_θ model are compared with the ones obtained with the κ-ϵ-κ_θ-ϵ_θ model and with DNS data from Kawamura database, see [3] and references therein. The fields in DNS data are usually reported in non dimensional form. The dimensionless temperature is defined as $\theta^+ = \theta/T_\tau$, where T_τ is the friction temperature calculated as $T_\tau = q/(u_\tau \rho C_p)$ and θ is the difference between the temperature and the linear behavior characteristic of the fully developed flow, $\theta = T - T_{w0} - x\,\Delta T_b$. T_{w0} is the reference inlet wall temperature which is assumed to be zero. By using the temperature θ instead of T we can impose periodic boundary conditions on θ when the flow is fully developed.

Seven simulations have been performed with Reynolds number of $Re \approx 5500$ (A), 13500 (B), 23250 (C), 40100 (D), 86200 (E), 203900 (F) and 344800 (G). They correspond to the friction Reynolds number of 180 (A), 395 (B), 640(C) , 1010 (D), 2000 (E), 4400 (F) and 7200 (G). A full report of these data can be found in [9, 10], where other data such as turbulent heat flux and turbulent Prandtl number are shown and a discussion over the use of different boundary conditions for the four parameter turbulence model is carried on. We remark the differences in convergence and stability of the solver for the two different turbulence models: the κ-ϵ solver needs a dt as time step for the transient solution which is ten to a hundred times smaller than the dt used for the κ-ω solver, otherwise no stable solution can be obtained. In Fig. 1 the non dimensional mean velocity profiles obtained with the κ-ω and with the κ-ϵ model $u^+ = \mathbf{u}/u_\tau$ are reported as a function of the non dimensional wall distance $y^+ = y u_\tau/\nu$ for two test cases, namely the case $Re \approx 5500$ (A) and $Re \approx 86200$ (E). The friction velocity u_τ is defined as $u_\tau = \sqrt{\tau_w/\rho}$ with τ_w the wall shear stress. The κ-ω model well reproduces the linear and logarithmic behaviors of the velocity, namely $u^+ = y^+$ and $u^+ = \log(y^+)/0.4 + 5$. Comparing the results obtained with κ-ω model with the ones obtained with κ-ϵ we can observe only a slight difference between them in the buffer region. In Fig. 2 the non dimensional temperature θ^+ is reported as a function of y^+ and divided by the Prandtl number. The temperature profiles for the cases $Re_\tau = 180$, $Re_\tau = 395$ and $Re_\tau = 640$, are compared with DNS data from Kawamura [3]. The data obtained with the four parameter models agree very well with the DNS ones. The non dimensional temperature profiles of all the simulated cases are reported in Fig. 3. The results obtained with the κ-ω-κ_θ-ω_θ, Fig. 3 (right), show no sensible differences with the κ-ϵ-κ_θ-ϵ_θ ones, Fig. 3 (left). The root-mean-square temperature fluctuation $\theta_{rms} = \sqrt{2\kappa_\theta}$ is an important variable needed to evaluate the time ratio R and the turbulent heat diffusion

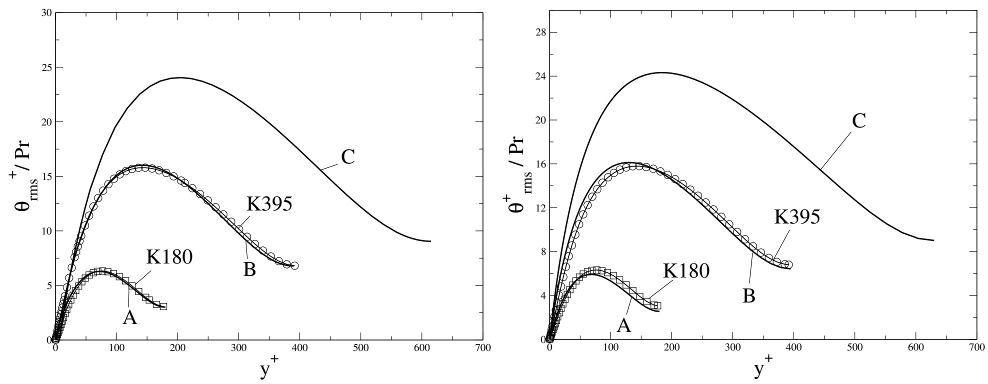

Figure 4. Plane case. The root-mean-square temperature fluctuations θ^+_{rms} for different $Re \approx 5500$ (A), 13500 (B), 23250 (C) and comparison with DNS corresponding data (K180) and (K395). On the left results with the κ-ϵ model, on the right κ-ω model.

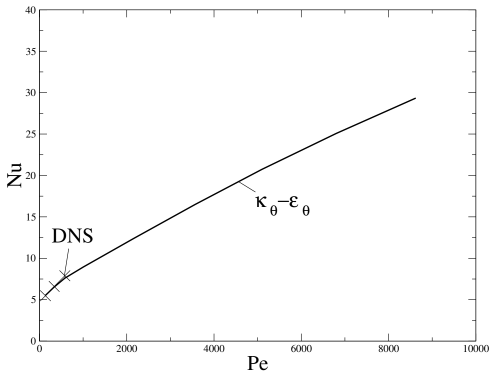

Figure 5. Plane case. Nusselt number (thick line) and DNS values (cross) for different Peclet numbers. On the left results with the κ-ϵ model, on the right κ-ω model.

coefficient α_t. In Fig. 4 the non dimensional $\theta^+_{rms} = \theta_{rms}/T_\tau$ is reported for the κ-ϵ (left) and κ-ω (right) formulation of the model and it is compared with DNS data for $Re_\tau = 180$ and 395. Very similar results to DNS data are obtained with both the turbulence models, a slight difference in the prediction of the position of the peak can be seen between the two models but the overall result is very good. The Nusselt number is the most important non dimensional number in engineering heat transfer calculations and it quantifies the heat transfer effectiveness. It is defined as $Nu = qD_h/(\lambda\Delta T)$ where D_h is the hydraulic diameter of the geometry and ΔT is the difference between the average wall temperature and the bulk temperature, defined as the average temperature on the section of the flow with respect to velocity. In Fig. 5 the Nusselt number calculated with the κ-ϵ (left) and κ-ω (right) four parameter turbulence models is reported as a function of Peclet number $Pe = Re\,Pr$. DNS data are reported as well for comparison. The first two points matches very well while the third (corresponding to $Re \approx 23250$ (C)) seems to slightly overestimate the DNS result.

3.2. Cylinder channel

As a second test we simulate a fully developed turbulent flow in a cylindrical pipe with diameter $D = 0.0605$. The physical properties of the simulated flow are reported in Table 1. For this geometrical case we compare our results with DNS data, which are available only for the case

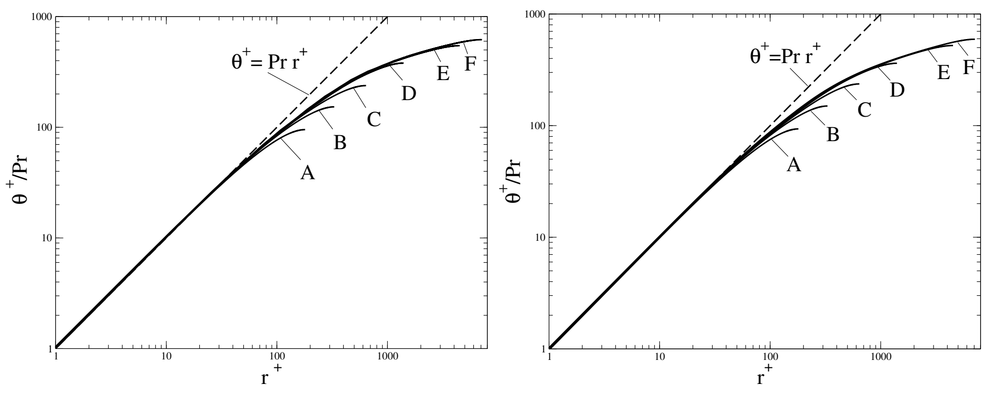

Figure 6. Cylinder case. Temperature distribution θ^+/Pr for $Re \approx 5500$ (A), 11150 (B), 23750 (C), 57500 (D), 213000 (E) and 345000 (F). Results obtained with κ-ϵ-κ_θ-ϵ_θ (left) and κ-ω-κ_θ-ω_θ (right) model.

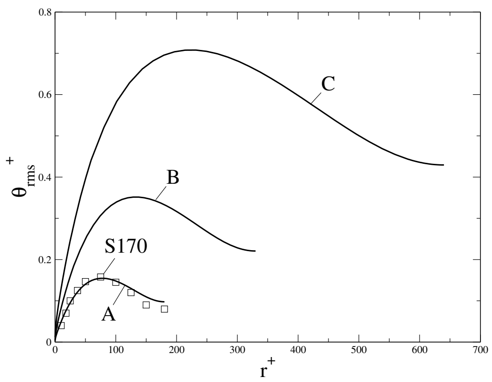

Figure 7. Cylinder case. Non-dimensional root-mean-square temperature fluctuation θ^+_{rms} for $Re \approx 5500$ (A), 11150 (B) and 23750 (C) and comparison with DNS data for $Re_\tau = 170$ (S170). On the left the results were obtained with the κ-ϵ model while on the right they were calculated with the κ-ω model.

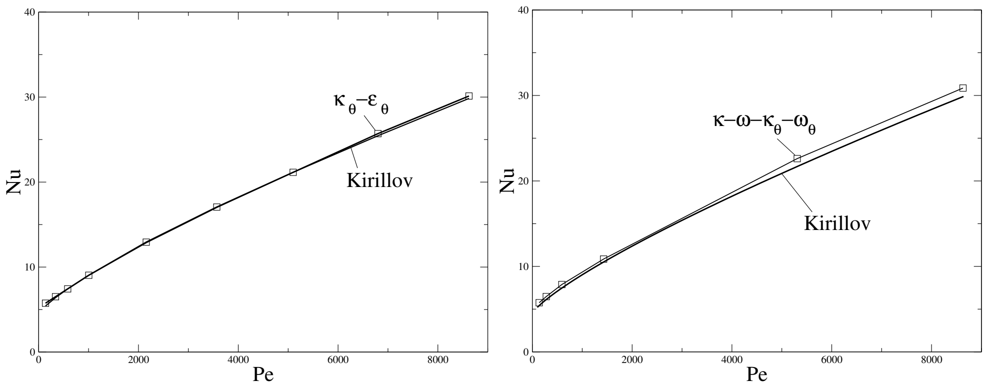

Figure 8. Cylinder case. Nusselt number (square) and Kirillov correlation for cylindrical geometry (thick line). On the left results obtained with the κ-ϵ model while on the right calculated with the κ-ω model.

$Re_\tau = 170$, and with the Kirillov heat transfer correlation

$$Nu = 4.5 + 0.018\, Pe^{0.8} \,. \tag{27}$$

This is the reference correlation for this class of fluids in cylindrical geometry [14, 15] and it is claimed to be valid for $10^4 < Re < 5 \cdot 10^6$.

We performed six simulations over a wide range of Reynolds numbers, namely $Re \approx 5500$ (A), 11150 (B), 23750 (C), 57500 (D), 213000 (E) and 345000 (F) corresponding to $Re_\tau = 180$ (A), 395 (B), 640 (C), 1400 (D), 4500 (E) and 7150 (F). The same behavior of the different solvers for κ-ϵ and κ-ω model as found for the plane cases is observed for the solution in these test cases. In Fig. 6 the non dimensional temperature divided by the Prandtl number θ^+/Pr is reported for all the simulated cases, as a function of the non dimensional wall distance $r^+ = ru_\tau/\nu$. Comparing Fig. 6 (right) with Fig. 6 (left) we can see that the κ-ω results are very close to the κ-ϵ ones. The linear behavior of the non dimensional temperature field is well reproduced in all the simulated cases. The non-dimensional root-mean-square temperature fluctuation θ^+_{rms} for $Re \approx 5500$ (A), 11150 (B) and 23750 (C) is compared with DNS data for $Re_\tau = 170$ (S170) in Fig. 7. A good agreement with the DNS data is obtained with both models. Comparing the κ-ϵ results with the κ-ω ones, for the cases $Re_\tau = 395$ and $Re_\tau = 640$ one can see some differences between the models but there are no reference results to compare with. The Nusselt number for these simulations is reported in Fig. 8. The square dots are the results obtained with the four parameter turbulence model, while the thick line is Kirillov correlation. On the left the results are reported for the κ-ϵ model while on the right for the κ-ω model. The matching between the numerical results and the correlation is almost perfect at any velocity for the κ-ϵ model while little discrepancies can be seen for the κ-ω model at very high velocities.

4. Conclusion

In this work we have proposed and analyzed an improved four parameter turbulence model for heat transfer computation of heavy liquid metal flows with $Pr \approx 0.025$. We have derived a κ-ω formulation from an already tested κ-ϵ turbulence model to obtain a more stable and robust model to compute turbulent heat transfer. The model has been tested in different geometries and a comparison with DNS data, experimental results and numerical results obtained with the κ-ϵ model has been performed. The results obtained show that the new κ-ω-κ_θ-ω_θ four parameter turbulence model is more stable and convergence obtained by using this model is faster. Moreover the comparison with DNS data and experimental results has proven that reliable results can be obtained with the new model, so it can be considered a useful tool in many engineering fields with heavy liquid metal applications.

References

[1] Cheng X and Tak N 2006 Investigation on turbulent heat transfer to lead-bismuth eutectic flows in circular tubes for nuclear applications *Nucl. Eng. Des.* **236** 385-93
[2] Cheng X and Tak N 2006 CFD analysis of thermal-hydraulic behavior of heavy liquid metals in sub-channels *Nucl. Eng. Des.* **236** 1874-85
[3] Kawamura H, Abe H and Matsuo Y 1999 DNS of turbulent heat transfer in channel flow with respect to Reynolds and Prandtl number effects *Int. J. Heat. Fluid. Fl.* **20** 196-207
[4] Hwang C B and Lin C A 1999 A low Reynolds number two-equation $k_t - e_t$ model to predict thermal field *Int. J. Heat. Mass Tran.* **42** 3217-30
[5] Nagano Y and Shimada M 1996 Development of a two equation heat transfer model based on direct simulations of turbulent flows with different Prandtl numbers Phys. Fluids **8** 3379-402
[6] Abe K, Kondoh T and Nagano Y 1995 A new turbulence model for predicting fluid flow and heat transfer in separating and reattaching flows II. Thermal field calculations *Int. J. Heat. Mass Tran.* **38** 1467-81
[7] Nagano Y, Pei C Q and Hattori H 1999 A new low-Reynolds-number one-equation model of turbulence *Flow Turbul. Combust.* **63** 135-51
[8] Abe K, Kondoh T and Nagano Y 1996 A two-equation heat transfer model reflecting second-moment closures for wall and free turbulent flows *Int. J. Heat. Fluid. Fl.* **17** 228-37
[9] Manservisi S and Menghini F 2014 A CFD four parameter heat transfer turbulence model for engineering applications in heavy liquid metals in rod bundle geometries *Int. J. Heat. Mass Tran.* **69** 312-26
[10] Manservisi S and Menghini F 2014 Triangular rod bundle simulations of a CFD κ-ϵ-κ_θ-ϵ_θ heat transfer turbulence model for heavy liquid metals *Nucl. Eng. Des.* **273** 251-70
[11] Hattori H, Nagano Y and Tagawa M 1993 Analysis of turbulent heat transfer under various thermal conditions with two-equation models *Eng. Turb. Mod. Exp.* **2** 43-52
[12] Launder B E, Reece G J and Rodi W 1975 Progress in the development of a Reynolds-stress turbulence closure *J. Fluid Mech.* **37** 537-66
[13] Deng B, Wu W and Xi S 2001 A near-wall two-equation heat transfer model for wall turbulent flow *Int. J. Heat. Mass Tran.* **44** 691-8
[14] Saha S, Chin C, Blackburn H M and Ooi A S H 2011 The influence of pipe length on thermal statistics computed from DNS of turbulent heat transfer *Int. J. Heat. Fluid. Fl.* **32** 1083-97
[15] Kirillov P and Ushakov P A 2001 Heat transfer to liquid metals: specific features, methods of investigation and main relationships *Therm. Eng.* **48** 50-9